Aligned synthesis of multi-walled carbon nanotubes with high purity by aerosol assisted chemical vapor deposition: Effect of water vapor

Hao Liu [a], Yong Zhang [a], Ruying Li [a], Xueliang Sun [a,*], Fengping Wang [b], Zhifeng Ding [b], Philippe Mérel [c], Sylvain Desilets [c]

[a] Department of Mechanical and Materials Engineering, The University of Western Ontario, London, ON N6A 5B9, Canada
[b] Department of Chemistry, The University of Western Ontario, London, ON N6A 5B7, Canada
[c] Defence Research & Development Canada-Valcartier, 2459 Boulevard Pie-XI nord, Québec, QC G3J 1X5, Canada

ARTICLE INFO

ABSTRACT

Aligned multi-walled carbon nanotubes (MWCNTs) with high purity and bulk yield were achieved on a silicon substrate by an aerosol-assisted chemical vapor deposition. The introduction of specific amounts of water vapor played a key role in *in situ* controlling the purity and surface defects of the nanotubes. The morphology, surface quality and structure of MWCNTs were characterized by secondary and backscattered electron imaging in a field emission scanning electron microscope (FESEM) and transmission electron microscope (TEM). Crystallinity and defects of the MWCNTs' were investigated by high-resolution transmission electron microscopy (HRTEM) and Raman spectroscopy. In this work, water vapor was found to provide a weak oxidative environment, which enhanced and purified the MWCNTs' growth. However, excessive water vapor would inhibit the MWCNTs growth with a poor surface quality. In addition, it has been found that the surface morphology of the CNTs can be modified intentionally through producing some surface defects by tuning the amount of the water vapor, which may offer more nucleation sites on the chemically inert CNT surface for various applications such as catalyst support.

1. Introduction

Since their discovery in 1991 [1], carbon nanotubes (CNTs) have exhibited great potentials in various applications, such as electron field emitter displays, nanoscale electronic devices, biosensors, hydrogen storage and fuel cell electrodes. Among various synthesis techniques, aerosol assisted chemical vapor deposition (AACVD) offers more opportunities for generating large volumes of CNTs with excellent areal selectivity, vertical alignment selectivity and selective doping with well-controlled stoichiometry [2]. However, a large amount of undesirable carbonaceous materials and impurity particles are always simultaneously involved in products accompanying the generation of CNTs due to contamination of solvent and chemical reagents, or those formed from precursors in the gas phase during AACVD, which severely degrade the performance of CNTs [3]. In order to achieve high quality CNTs, post-purification such as oxidations [4,5] and hydrothermal treatments [6] have been employed. Compared to post-purification processes, an *in situ* purifying strategy is increasingly attractive due to its high efficiency and low cost [7]. Recently mild oxidizing agents (e.g. water vapor) have been introduced to induce the so-called "super growth" of

single-walled CNTs [8–10]. However, few reports have focused on the effect of weak oxidizing agent on the synthesis of MWCNTs, which exhibit more promising potential in some applications such as catalyst support, due to their established high electrical conductivity.

In the present work, aligned synthesis of MWCNTs with high purity (low impurity particles and carbonaceous materials) has been obtained in an AACVD process via an *in situ* weak oxidation method. Further, it has been reported that CNTs with appropriate defects can bestow high metal adsorption capability in aqueous solution because of the functional groups attached on their surfaces [11,12]. We found that the surface morphology of the CNTs can be modified intentionally through producing some surface defects by tuning the amount of the introduced water vapor, which may offer more nucleation sites on the chemically inert CNTs surface for the future catalyst deposition [13].

2. Experimental method

The synthesis of MWCNTs was carried out by a purpose-built aerosol assisted CVD (AACVD) system that has been reported elsewhere [14]. Briefly, the method is based on the decomposition of an aerosol consisting of a liquid hydrocarbon source and an evaporable catalyst for the CNTs growth. A 30 nm-thick aluminum
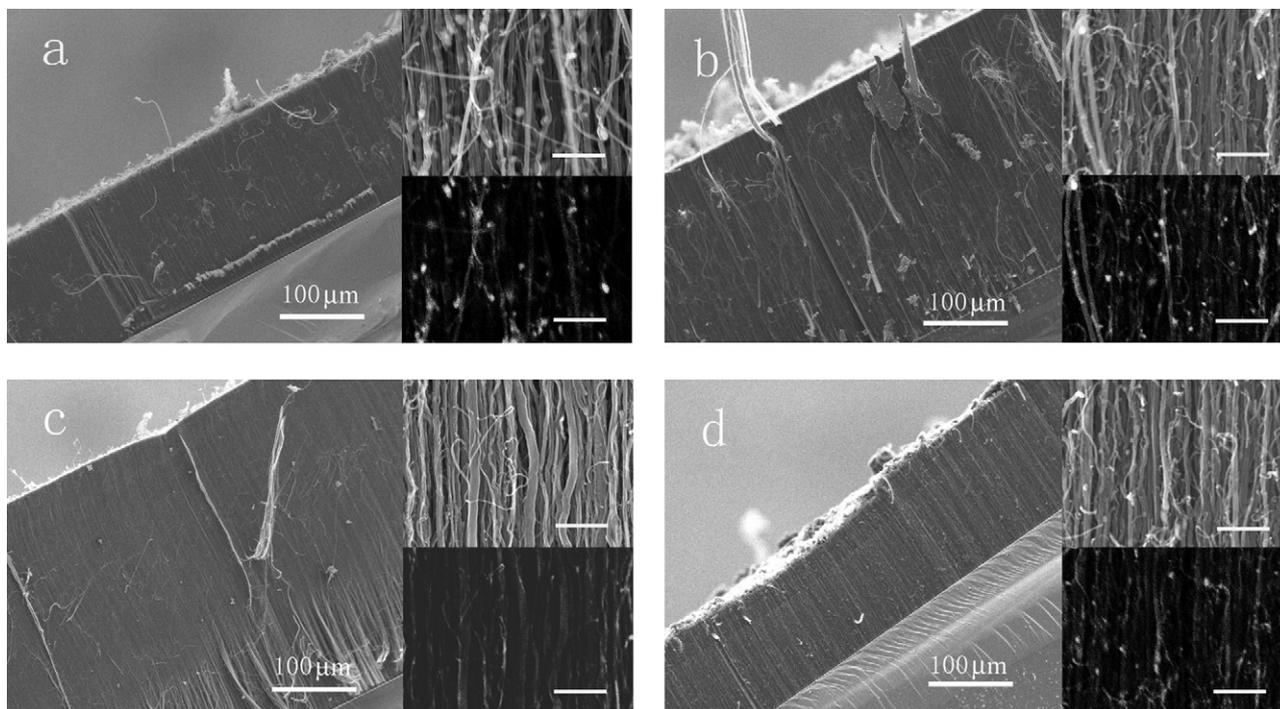
Fig. 1. SEM images of CNTs showing water effects (a) without water, (b) a little wet argon (10 sccm), (c) optimized amount of wet argon (150 sccm), and (d) excessive wet argon (700 sccm). All scale bars in inserted images are 500 nm. In each image, the bigger left image is low magnification SEM image, the up-right corner one is high magnification SEM image and the down-right corner one is back scattered electron image.

buffer layer was sputtered onto a silicon wafer with a 600 nm-thick SiO_2 layer. The silicon substrate was set in a ceramic boat, and the substrate/boat assembly was placed inside the chamber. After 20-min-evacuation of the air, the furnace was heated to 850 °C within 15 min. As soon as the temperature reached 850 °C, the aerosol droplets were produced by ultrasonication and transported by argon gas with a flow rate of 1500 sccm. Diluting argon gas was introduced from two additional inlets at a flow rate of a further 700 sccm in total. Keeping the total argon flow rate unchanged, introduction and amount control of water vapor was realized by tuning the flow rate of argon which passed through a water bubbler from one of the two additional inlets. Meanwhile, hydrogen was introduced through a fourth inlet with a flow rate of 1800 sccm. The growth time was 30 min.

The samples were characterized by various analysis techniques including Hitachi S-4800 field-emission scanning electron microscope (SEM) operated at 5.0 kV, Philips CM10 transmission electron microscope (TEM) operated at 80 kV, JEOL 2010F transmission electron microscope (TEM) operated at 200 kV, and a Horiba Jobin Yvon high resolution (HR800) confocal Raman spectrometer operated with an incident laser beam at 632.8 nm.

3. Results and discussion

Fig. 1 shows cross-sectional SEM images of the as-synthesized CNTs. The lengths of the aligned CNTs are approximately 150 μm, 300 μm, 400 μm and 150 μm with the wet argon flow rates of 0, 10, 150 and 700 sccm, respectively. In each image, the left image is low magnification SEM image, the up-right corner one is higher magnification secondary electron SEM image and the down-right corner one is the corresponding backscattered electron image.

The close SEM examinations reveal that all synthesized CNTs are perpendicular to the substrate. Without water vapor, shown in Fig. 1a, lots of catalyst particles are observed either inside the CNTs or clinging to the outer surface. With 10 sccm wet argon as shown in Fig. 1b, the surface of the synthesized CNTs is cleaner than

the ones without water. However, the backscattered electron SEM image shows that there are still several catalyst particles inside the CNTs other than clinging to the outside layer. As the wet argon flow rate increases to 150 sccm as shown in Fig. 1c, hardly any particles can be observed inside or outside our CNTs, revealing that the quality of CNTs is greatly improved with the introduction of the oxidative wet argon. The secondary electron SEM and backscattered SEM images of the CNTs synthesized with 700 sccm wet argon in Fig. 1d show that the CNTs are not as straight as other tubes and catalyst particles appear both inside and outside CNTs.

In order to investigate the effect of water vapor on the CNTs growth, systematic experiments have been conducted under different flow rates of wet argon from 10 to 700 sccm. Based on our SEM data, a correlation between the growth rate and the wet argon flow rate is plotted in Fig. 2. The growth rate of CNTs reached its maximum when the flow rate of wet argon was controlled in the range of 100–150 sccm. When the flow rate of wet argon was increased beyond 200 sccm, the growth of CNTs was evidently restricted as
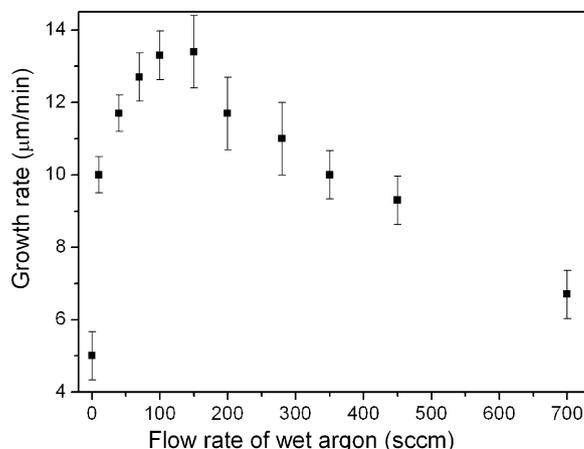
Fig. 2. Growth rate of MWCNTs as a function of flow rate of wet argon.
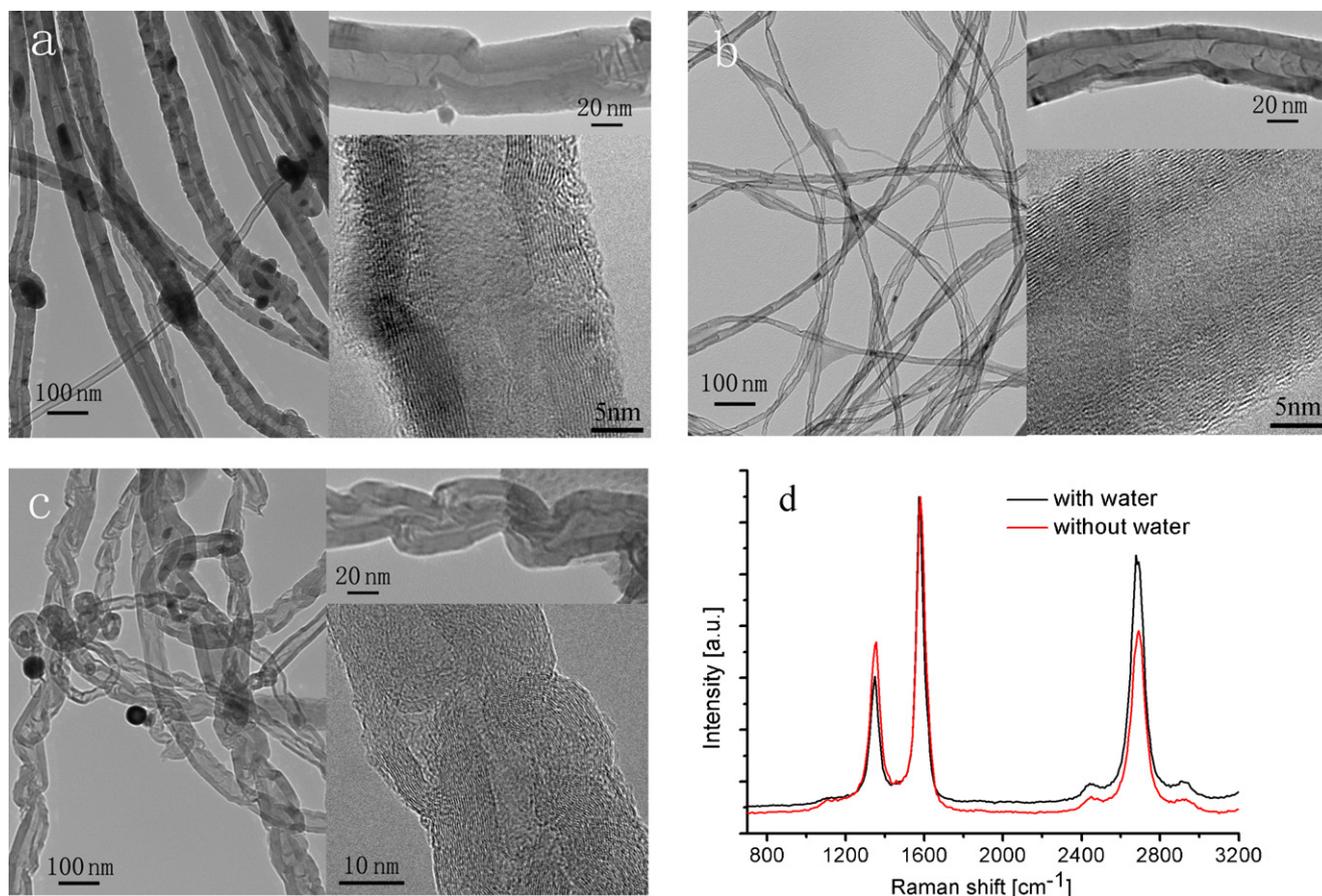
Fig. 3. TEM images and Raman spectra of CNTs using different wet argon flows. (a) Dry argon, (b) 150 sccm wet argon, (c) 700 sccm wet argon, and (d) Raman spectra of CNTs with dry argon and 150 sccm wet argon.

shown in Fig. 2. According to the previous report, CNTs growth suffers from the generation of amorphous carbon on the surface of the catalyst particle, which deteriorates the activity and lifetime of the catalyst and hinders the nanotube growth [3]. When an appropriate amount of water vapor was introduced into the system, the amorphous carbon was etched away through selective oxidation reactions with the water vapor and the lifetime of active catalyst particles could be extended [8,9]. Therefore, the growth rate of the CNTs was significantly enhanced. However, it is crucial to control the relative level of water and hydrocarbon (m-xylene was used here) to optimize the growth rate of the CNTs. With further increase of the water vapor amount, diffusion and penetration of m-xylene through the nanotube bundles were lessened and it was more and more difficult for the m-xylene molecules to reach the catalysts. Consequently, the height of the CNTs was reduced.

To get insight into detailed structure of the CNTs, the samples were examined by TEM and HRTEM. As shown in Fig. 3a, there are some particles clinging to the surface of the CNTs when they were synthesized with dry argon. The average diameter of the CNTs is about 60 nm. Some defects are observed on the graphitic layers, and an evident amorphous carbon layer of about 2 nm is observed on the CNTs surface and the walls of CNTs are curved with the adhesion of catalyst particles, shown in inserted HRTEM image. In this case, almost all graphite layers are parallel. When 150 sccm wet argon was used, the TEM images in Fig. 3b show that the nanotube diameter is reduced to 40 nm and the walls of the CNTs become thinner. Meanwhile, more curved defective structures are observed along the tubes. The HRTEM image inserted in Fig. 3b shows that the first several outer layers of the nanotube display lower crystallinity compared to the inner layers. Furthermore, most of the

outer surface of the tube wall is free of amorphous carbon layers. When the wet argon flow rate reached 700 sccm shown in Fig. 3c, ordered structures are destroyed and large numbers of defects are presented in the cylindrical graphitic sheets, which resulted in a lower crystallinity. Our systematic TEM investigation (not shown) has indicated that the defect increases with increasing water vapor amount. Although there are many defects that curl the CNTs, the CNTs are still aligned because of the mutual support effect provided by adjacent CNTs. The HRTEM image shows that many small defects (instead of amorphous carbon) are observed on the surface of CNTs, and that crystallinity declines.

From the TEM and HRTEM observations, the amorphous carbon and particles clinging on the surface of the CNTs decrease as the addition of wet argon increases, while this oxidative gas also increases crystallization defects of the graphene structure. Consequently, the structural defects of the CNTs can be controlled by modulating the amount of wet argon. Evidently, water vapor played an essential role in removing the amorphous carbon by weak oxidation effect during the CNTs growth. On the other hand, metal particles could enhance the oxidation of carbon contacting with the particles at the reaction temperature [15], which may both assist the water vapor against the amorphous carbon and reduce the chances of the metal particles to cling on the nanotube surface. Therefore, CNTs with clean morphology, amorphous carbon free and different defect amount could be obtained by balancing the level of water to m-xylene. In addition, the controlled level of water to m-xylene ensured continuous and stable growth of the CNTs by tuning the activity and lifetime of the catalyst and thereafter balancing the rate of carbon supply and that of solid carbon precipitation as well. Maybe that is one of the reasons why

hardly any particles were observed inside the CNTs at the proper amount of the water vapor. When the water content was raised to a high level, the excessive water vapor would lead to the discontinuous supply of carbon source to the catalyst as discussed above. In this case, it was difficult to keep the balance between the carbon supply and the solid carbon precipitation. Consequently, distorted CNTs with high level defects were grown, which provided more sites for metal particles to attach and some catalyst particles reappeared on the CNTs. This is in consistent with our SEM and TEM observation.

We also used Raman spectroscopy to evaluate the quality of the CNTs in terms of the crystallinity and defects in the absence or presence of water vapor. Two representative Raman spectra are shown here for the samples grown under dry argon and the optimized 150 sccm wet argon (Fig. 3d). Both spectra present three bands at $\sim$1355 cm^{-1} (D band), attributed to defects such as pentagons in graphite and amorphous carbon [16,17], $\sim$1580 cm^{-1} (G band), indicating the formation of well graphitized carbon tubes, and $\sim$2690 cm^{-1} (G$'$ band), known as indication of clean samples [17]. As shown in Fig. 3d, the intensity ratio of D band to G band (I_D/I_G) decreases from 0.54 to 0.41 for the samples grown under dry and wet argon, respectively. This indicates the degree of long-range ordered crystalline perfection of the CNTs increased when water vapor was introduced into the reaction chamber. Structures with pentagons, heptagons and amorphous carbon were etched away first by the selective oxidation [3,5]. This result is consistent with the TEM observation that catalysts on the surface of CNTs disappeared in indirect proportion to the addition of water, which greatly reduced the defects. The ratio of G$'$ band to G band ($I_{G'}/I_G$) is also calculated to estimate the quality of the CNTs. The $I_{G'}/I_G$ increases from 0.57 to 0.81 with the introduction of water vapor, indicating a lower amount of carbonaceous impurity [18] in the CNTs when the water vapor was involved in the growth process. This agrees with the result from I_D/I_G analysis. Frequency width at half maximum (FWHM) in the Raman spectrum has been considered as a criterion in evaluating the structural disorder of CNTs, which arises from bond angle and bond length distortions [19]. The FWHM of the D band, G band and G$'$ band (FWHM (D), FWHM (G) and FWHM (G$'$)) for CNTs growing without water are 60, 53 and 81, respectively, which are a little wider than those for CNTs growing with water i.e. 50, 46 and 81. It is obvious that introduction of water vapor narrowed down the FWHM (D) and FWHM (G) but left FWHM (G$'$) unchanged. This is consistent with our observation that the CNTs grown with water vapor have less disordered bonds and amorphous carbon since the FWHM (D) has the same tendency as I_D/I_G [20]. Therefore, the spectra show great consistency to support the hypothesis that the addition of water during the growing process is an effective way to get high quality CNTs. When the flow rate of wet argon was increased to 700 sccm, the Raman spectrum shows only one wide band between 1200 cm^{-1} and 2000 cm^{-1} (not shown), due to the distortion of graphene layers. We can conclude that an oxidative atmosphere has at least two effects on the growth of CNTs, i.e. the purification of CNTs by oxidizing the amorphous layer and the disfiguration of CNTs by destroying the graphene layers. The former effect can increase the crystallinity of the CNTs while the latter one has a negative influence on the crystallinity.

Therefore, it can be concluded that the growth of purified and defect-controlled CNTs can be realized by introducing appropriate amount of oxidative water vapor. The CNTs as supporting materials will have great potentials in catalysts and adsorption applications. For instance, as an attractive adsorbent, CNTs have been targeted to remove trace pollutants such as Zn^{2+} [11], Cd^{2+} [21], Pb^{2+} [22], Cu^{2+} [23] and Cr^{6+} [24] from water. The purposely introduced surface defects of the CNTs would provide preferable sites for catalyst deposition.

4. Conclusion

A detailed investigation on the purity and structure control of MWCNTs was conducted in the present work. The water vapor effect on the CNTs growth was determined by SEM, TEM, HRTEM and Raman spectroscopy. The crystallinity was improved with the introduction of wet argon at first and then deteriorated with the excessive wet argon amount. The carbonaceous impurities covering the tube walls were reduced substantially with an optimized amount of water vapor and some defect structures could be intentionally produced on the CNTs surface. The CNTs produced in the optimum conditions have great potentials for various applications such as electrodes in fuel cell, catalyst supports and sensors.

References

[1] Y.Q. Xu, H. Peng, R.H. Hauge, R.E. Smalley, Controlled multistep purification of single-walled carbon nanotubes, Nano Lett. 5 (2005) 163–168.
[2] X. Hou, K.-L. Choy, Processing and applications of aerosol-assisted chemical vapor deposition, Chem. Vap. Depos. 12 (2006) 583–596.
[3] J.-S. Lee, A. Chandrashekar, B.M. Park, L.J. Overzet, G.S. Lee, Effects of oxygen plasma on optical and electrical characteristics of multiwall carbon nanotubes grown on a four-probe patterned Fe layer, J. Vac. Sci. Technol. B 23 (2005) 1013–1017.
[4] D. Porwal, K. Mukhopadhyay, K. Ram, G.N. Mathur, Investigation of the synthesis strategy of CNTs from CCVD by thermal analysis, Thermochim. Acta 463 (2007) 53–59.
[5] Y.S. Park, Y.C. Choi, K.S. Kim, D.-C. Chung, D.J. Bae, K.H. An, S.C. Lim, X.Y. Zhu, Y.H. Lee, High yield purification of multiwalled carbon nanotubes by selective oxidation during thermal annealing, Carbon 39 (2001) 655–661.
[6] K. Tohji, H. Takahashi, Y. Shinoda, N. Shimizu, B. Jeyadevan, I. Matsuoka, Purification procedure for single-walled nanotubes, J. Phys. Chem. B 101 (2007) 1974–1978.
[7] A. Cao, X. Zhang, C. Xu, J. Liang, D. Wu, B. Wei, Aligned carbon nanotube growth under oxidative ambient, J. Mater. Res. 16 (2001) 3107–3110.
[8] P.B. Amama, C.L. Pint, L. McJilton, S.M. Kim, E.A. Stach, P.T. Murray, R.H. Hauge, B. Maruyama, Role of water in super growth of single-walled carbon nanotube carpets, Nano Lett. 9 (2009) 44–49.
[9] J.L. Hu, C.C. Yang, J.H. Huang, Vertically-aligned carbon nanotubes prepared by water-assisted chemical vapor deposition, Diamond Relat. Mater. 17 (2008) 2084–2088.
[10] C.L. Pint, S.T. Pheasant, A.N.G. Parra-Vasquez, C. Horton, Y. Xu, R.H. Hauge, Investigation of optimal parameters for oxide-assisted growth of vertically aligned single-walled carbon nanotubes, J. Phys. Chem. C 113 (2009) 4125–4133.
[11] C. Lu, H. Chiu, Adsorption of zinc (II) from water with purified carbon nanotubes, Chem. Eng. Sci. 61 (2006) 1138–1145.
[12] H.J. Wang, A.L. Zhou, F. Peng, H. Yu, L.F. Chen, Adsorption characteristic of acidified carbon nanotubes for heavy metal Pb(II) in aqueous solution, Mater. Sci. Eng. A 466 (2007) 201–206.
[13] C. Bittencourt, M. Hecq, A. Felten, J.J. Pireaux, J. Ghijsen, M.P. Felicissimo, P. Rudolf, W. Drube, X. Ke, G. Van Tendeloo, Platinum–carbon nanotube interaction, Chem. Phys. Lett. 462 (2008) 260–264.
[14] Y. Zhang, R. Li, H. Liu, X. Sun, P. Merel, S. Desilet, Integration and characterization of aligned crbon nanotubes on metal/silicon substrates and effects of water, Appl. Surf. Sci. 255 (2009) 5003–5008.
[15] K. Hata, D.N. Futaba, K. Mizuno, T. Namai, M. Yumura, S. Iijima, Water-assisted highly efficient synthesis of impurity-free single-walled carbon nanotubes, Science 306 (2004) 1362–1364.
[16] H. Hiura, T.W. Ebbesen, K. Tanigaki, H. Takahashi, Raman studies of carbon nanotubes, Chem. Phys. Lett. 202 (1993) 509–512.
[17] C.C. Chuang, J.H. Huang, W.J. Chen, C.C. Lee, Y.Y. Chang, Role of amorphous carbon nanowires in reducing the turn-on field of carbon films prepared by microwave-heated CVD, Diamond Relat. Mater. 13 (2004) 1012–1016.
[18] R.A. DiLeo, B.J. Landi, R.P. Raffaelle, Purity assessment of multiwalled carbon nanotubes by Raman spectroscopy, J. Appl. Phys. 101 (2007) 0643071–0643074.
[19] C. Casiraghi, A.C. Ferrari, J. Robertson, Raman spectroscopy of hydrogenated amorphous carbons, Phys. Rev. B 72 (2005) 0854011–08540114.

[20] E.F. Antunes, A.O. Lobo, E.J. Corat, V.J. Trava-airoldi, Influence of diameter in the Raman spectra of aligned multi-walled carbon nanotubes, Carbon 45 (2007) 913–921.

[21] Y.H. Li, S. Wang, Z. Luan, J. Ding, C. Xu, Adsorption of cadmium(II) from aqueous solution by surface oxidized carbon nanotubes, Carbon 41 (2003) 1057–1062.

[22] Y.H. Li, Y. Zhu, Y. Zhao, D. Wu, Z. Luan, Different morphologies of carbon nanotubes effect on the lead removal from aqueous solution, Diamond Relat. Mater. 15 (2006) 90–94.

[23] C.H. Wu, Studies of the equilibrium and thermodynamics of the adsorption of Cu^{2+} onto as-produced and modified carbon nanotubes, J. Colloid Interface Sci. 311 (2007) 338–346.

[24] Z.C. Di, J. Ding, X.J. Peng, Y.H. Li, Z. Luan, J. Liang, Chromium adsorption by aligned carbon nanotubes supported ceria nanoparticles, Chemosphere 62 (2006) 861–865.